5 August 2002

PHYSICS LETTERS A

ELSEVIER

Physics Letters A 300 (2002) 385–391

www.elsevier.com/locate/pla

Electrorotation of colloidal suspensions

J.P. Huang [a], K.W. Yu [a,*], G.Q. Gu [a,b]

[a] *Department of Physics, The Chinese University of Hong Kong, Shatin, NT, Hong Kong*
[b] *College of Information Science and Technology, East China Normal University, Shanghai 200 062, China*

Received 27 February 2002; received in revised form 6 June 2002; accepted 7 June 2002

Communicated by C.R. Doering

Abstract

When a strong electric field is applied to a colloidal suspension, it may cause an aggregation of the suspended particles in response to the field. In the case of a rotating field, the electrorotation (ER) spectrum can be modified further due to the local field effects arising from the many-particle system. To capture the local field effect, we invoke the Maxwell–Garnett approximation for the dielectric response. The hydrodynamic interactions between the suspended particles can also modify the spin friction, which is a key to determine the angular velocity of ER. By invoking the spectral representation approach, we derive the analytic expressions for the characteristic frequency at which the maximum angular velocity of ER occurs. From the numerical calculation, we find that there exist two sub-dispersions in the ER spectrum. However, the two characteristic frequencies are so close that the two peaks actually overlap and become a single broad peak. We report a detailed investigation of the dependence of the characteristic frequency and the dispersion strength of ER on various material parameters. © 2002 Elsevier Science B.V. All rights reserved.

PACS: 82.70.-y; 87.22.Bt; 77.22.Gm; 77.84.Nh

1. Introduction

AC electrokinetic phenomena, such as dielectrophoresis and electrorotation (ER) have been investigated to yield the selective manipulation and characterization of biological cells. Under the action of external fields, colloidal particles or biological cells in suspensions exhibit rich fluid-dynamic behavior as well as dielectric response. It is also interesting to investigate their frequency-dependent responses to ac fields, which leads to valuable information on the structural (Maxwell–Wagner) polarization effects [1,2]. The polarization is characterized by a variety of characteristic frequency-dependent changes known as dielectric dispersion.

In the last two decades, various experimental tools have been developed to analyze the polarization of biological cells—dielectric spectroscopy [3], dielectrophoresis [4] and ER [5] techniques. Among these techniques, conventional dielectrophoresis and ER are usually applied to analyze the frequency dependence of translations and rotations of cells in a rotating electric field, respectively [4,5]. Moreover, one is able to monitor the cell movements with the aid of automated video analysis [6] as well as light scattering methods [2]. In ER, a dipole moment is induced in response

* Corresponding author.
E-mail address: kwyu@sun1.phy.cuhk.edu.hk (K.W. Yu).

0375-9601/02/$ – see front matter © 2002 Elsevier Science B.V. All rights reserved.
PII: S0375-9601(02)00850-2

to the rotating field. Then any dispersion process is able to cause a phase shift between the induced dipole moment and the external field vector, resulting in a desired torque which causes the cells to rotate.

In the dilute limit, the ER of individual cell can be predicted by ignoring the mutual interaction between cells. However, the cells may be aggregated under the influence of the external field. In this case the Brownian motion can be neglected, and thus the system becomes nondilute even though it is initially dilute. Then the role of mutual interaction will become dominant. As an initial model, we studied the ER of two approaching spherical particles in the presence of a rotating electric field in a recent paper [7]. We showed that when the two particles approach and finally touch, the mutual polarization interaction between the particles leads to a change in the dipole moment of individual particles and hence the ER spectrum, as compared to that of isolated particles. The mutual polarization effects were captured via the multiple image method [8]. From the results, we found that the mutual polarization effects can lower the characteristic frequency at which the maximum ER angular velocity occurs.

When the volume fraction of the suspension becomes large, the mutual interactions between the suspended particles can also modify the spin friction, which is a key to determine the angular velocity of ER. For ER of two particles in a rotating electric field, we have successfully applied the spectral representation to calculate the dispersion frequency. However, the determination of the spin friction was lacking.

For two particles, the basic tool is the reflection method [9], being analogous to the multiple image method in electrostatics, but being valid for two particles only. For more than two particles, we need a first-principles method, e.g., the Green's function (Oseen tensor) formulation. For a dilute suspension, however, one may adopt the effective medium theories [10] to capture the effective viscosity of a suspension. Thus, in this case, the ER spectrum can be modified further.

Regarding the spectral representation approach [11], it is a rigorous mathematical formalism of the effective dielectric constant of a two-phase composite material. It offers the advantage of the separation of material parameters (namely the dielectric constant and conductivity) from the particle structure information, thus simplifying the study. In the present work, we will derive the analytic expressions for the characteristic frequencies by using the spectral representation approach.

2. Formalism

We consider homogeneous, spherical particles exposed to a rotating electric field of frequency f, in which particles of complex dielectric constant $\tilde{\epsilon}_1 = \epsilon_1 + \sigma_1/(i2\pi f)$ are dispersed in a suspension of $\tilde{\epsilon}_2 = \epsilon_2 + \sigma_2/(i2\pi f)$, with $i = \sqrt{-1}$. Here, ϵ_i and σ_i represent the dielectric constant and conductivity, respectively.

For the effective dielectric constant $\tilde{\epsilon}_e$ of the whole system, we have

$$\frac{\tilde{\epsilon}_e - \tilde{\epsilon}_2}{\tilde{\epsilon}_e + 2\tilde{\epsilon}_2} = p\frac{\tilde{\epsilon}_1 - \tilde{\epsilon}_2}{\tilde{\epsilon}_1 + 2\tilde{\epsilon}_2}, \tag{1}$$

where p is the volume fraction of particles. Note that the $p = 0$ limit throughout the Letter is just the isolated spherical result [7]. In this case, the dipole factor of the particle is given by

$$b = \frac{\tilde{\epsilon}_1 - \tilde{\epsilon}_e}{\tilde{\epsilon}_1 + 2\tilde{\epsilon}_e}. \tag{2}$$

In order to obtain the analytic expression for the characteristic frequency, we resort to the spectral representation approach. By introducing a material parameter

$$\tilde{s} = \left(1 - \frac{\tilde{\epsilon}_1}{\tilde{\epsilon}_2}\right)^{-1},$$

Eq. (2) admits the form

$$b = \frac{F_1}{\tilde{s} - s_1} + \frac{F_2}{\tilde{s} - s_2}, \tag{3}$$

where

$$F_1 = -\frac{(1-p)(\sqrt{8+p} - \sqrt{p})}{6\sqrt{8+p}},$$

$$F_2 = -\frac{(1-p)(\sqrt{8+p} + \sqrt{p})}{6\sqrt{8+p}},$$

$$s_1 = \frac{1}{6}\big(2 + p - \sqrt{p(8+p)}\big),$$

$$s_2 = \frac{1}{6}\big(2 + p + \sqrt{p(8+p)}\big).$$

After some simple manipulations, Eq. (3) becomes [7,12]

$$b = \frac{F_1}{s - s_1} + \frac{\Delta\epsilon_1}{1 + if/f_{c1}} + \frac{F_2}{s - s_2} + \frac{\Delta\epsilon_2}{1 + if/f_{c2}}, \tag{4}$$

where the dispersion magnitudes $\Delta\epsilon$ and characteristic frequencies f_c being given by

$$\Delta\epsilon_1 = F_1 \frac{s - t}{(t - s_1)(s - s_1)},$$
$$\Delta\epsilon_2 = F_2 \frac{s - t}{(t - s_2)(s - s_2)},$$
$$f_{c1} = \frac{1}{2\pi} \frac{\sigma_2 s(t - s_1)}{\epsilon_2 t(s - s_1)},$$
$$f_{c2} = \frac{1}{2\pi} \frac{\sigma_2 s(t - s_2)}{\epsilon_2 t(s - s_2)},$$

and $s = 1/(1 - \epsilon_1/\epsilon_2)$ and $t = 1/(1 - \sigma_1/\sigma_2)$ are the dielectric and conductivity contrasts, respectively. Note that we predict two characteristic frequencies f_{c1} and f_{c2}.

Regarding the dynamic viscosity, the noninteracting spin friction expression for an isolated spherical particle must be modified. For many particles interacting in a suspension, we must consider the suspension hydrodynamics. The spin friction is calculated by considering the hydrodynamics of a rotating particle in a homogeneous suspension with an effective viscosity η_e. The effective viscosity for a suspension may be obtained from an analogous Maxwell–Garnett approximation (MGA) [10]

$$\frac{\eta_e - \eta_2}{\eta_e + \frac{3}{2}\eta_2} = p \frac{\eta_1 - \eta_2}{\eta_1 + \frac{3}{2}\eta_2}, \tag{5}$$

where η_1 and η_2 are respectively the viscosity of particle and host, and we may take $\eta_1 \to \infty$ for hard spheres. The dilute limit expression for the effective viscosity is

$$\eta_e = \eta_2 + \left(\frac{5}{2}p\right)\eta_2 + \left(\frac{5}{2}p^2\right)\eta_2 + \cdots. \tag{6}$$

This equation is a suitable method to determine the effective viscosity at low concentration as it predicts no percolation threshold. The effective medium approximation (EMA) is also a useful method to evaluate the effective viscosity of a suspension, which admits the form [10]

$$p \frac{\eta_1 - \eta_e}{\eta_1 + \frac{3}{2}\eta_e} + (1 - p) \frac{\eta_2 - \eta_e}{\eta_2 + \frac{3}{2}\eta_e} = 0. \tag{7}$$

We should remark that a percolation threshold $p_c = 0.4$ is predicted by Eq. (7). From this equation, the dilute limit expression is

$$\eta_e = \eta_2 + \left(\frac{5}{2}p\right)\eta_2 + \left(\frac{5}{2}p\right)^2\eta_2 + \cdots. \tag{8}$$

To one's interest, Eqs. (6) and (8) attain the same expansion up to first order in p. In addition, we should also remark that both Eqs. (5) and (7) are valid only at low Reynolds number.

It is known that the rotational angular velocity of a particle is related to the dipole factor as follows

$$\Omega(f) = -\frac{\epsilon_e E_0^2}{2\eta_e} \operatorname{Im}[b], \tag{9}$$

where E_0 is the strength of the applied electric field, and Im$[\cdots]$ means taking the imaginary part of $[\cdots]$.

3. Numerical results

During the numerical calculation, set $E_0 = 1.0 \times 10^4$ V/m, $\eta_2 = 1.0 \times 10^{-3}$ Kg/(m s). Note ϵ_0 denotes the dielectric constant of free space.

Fig. 1(a) is plotted versus frequency f for three different ϵ_1 at $\sigma_2 = 2.8 \times 10^{-4}$ S/m, $\epsilon_2 = 80\epsilon_0$, $p = 0.05$ and $\sigma_1 = 2.8 \times 10^{-2}$ S/m. Given ϵ_1, there is always one peak for angular velocity as frequency increases. The frequency located by the peak is just the characteristic frequency. We should remark here that two peaks we predict above are located so close that only one peak behavior is shown. In our previous work [7], a pair of particles is investigated by considering the mutual depolarization effect, and we found that one peak is dominant while the other has a lower value and is located in a quite different position. This shows that the particle aggregation effect may enhance the second peak value, and be relocated close to the dominant one. Regarding the related quantitative explanation, please refer to Fig. 3 arising from the spectral representation approach. As ϵ_1 increases, both the characteristic frequency and the angular-velocity peak value decreases.

Fig. 1(b) is plotted versus frequency f for three different ϵ_2 at $\sigma_2 = 2.8 \times 10^{-4}$ S/m, $p = 0.05$,

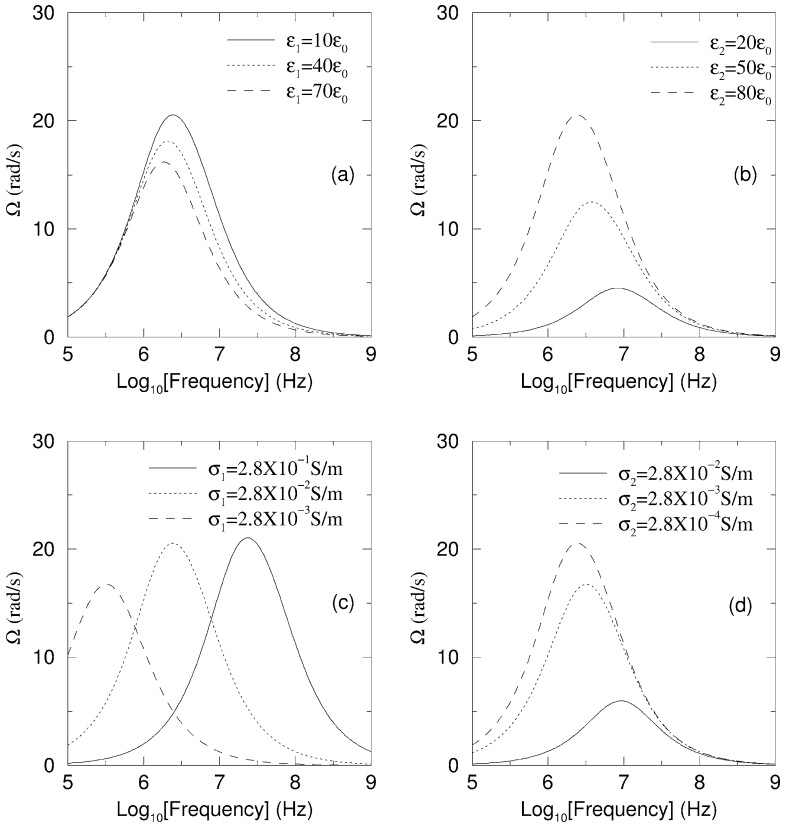

Fig. 1. Dependence of rotational angular velocity on ϵ_1, ϵ_2, σ_1 and σ_2 versus frequency (for the MGA only). (a) $\sigma_2 = 2.8 \times 10^{-4}$ S/m, $\epsilon_2 = 80\epsilon_0$, $p = 0.05$ and $\sigma_1 = 2.8 \times 10^{-2}$ S/m. (b) $\sigma_2 = 2.8 \times 10^{-4}$ S/m, $p = 0.05$ and $\epsilon_1 = 10\epsilon_0$ and $\sigma_1 = 2.8 \times 10^{-2}$ S/m. (c) $\sigma_2 = 2.8 \times 10^{-4}$ S/m, $\epsilon_2 = 80\epsilon_0$, $p = 0.05$ and $\epsilon_1 = 10\epsilon_0$. (d) $\epsilon_2 = 80\epsilon_0$, $p = 0.05$ and $\epsilon_1 = 10\epsilon_0$ and $\sigma_1 = 2.8 \times 10^{-2}$ S/m.

$\epsilon_1 = 10\epsilon_0$ and $\sigma_1 = 2.8 \times 10^{-2}$ S/m. It is evident that increasing ϵ_2 yields decreasing characteristic frequency, but increasing angular-velocity peak value.

Fig. 1(c) is plotted versus frequency f for three different σ_1 at $\sigma_2 = 2.8 \times 10^{-4}$ S/m, $\epsilon_2 = 80\epsilon_0$, $p = 0.05$ and $\epsilon_1 = 10\epsilon_0$. It is evident that both the characteristic frequency and the angular-velocity peak value increase for increasing σ_1.

Fig. 1(d) is plotted versus frequency f for three different σ_2 at $\epsilon_2 = 80\epsilon_0$, $p = 0.05$ and $\epsilon_1 = 10\epsilon_0$ and $\sigma_1 = 2.8 \times 10^{-2}$ S/m. For an increasing σ_2, the characteristic frequency increases whereas the angular-velocity peak value decreases concomitantly.

In Fig. 2, the effect of volume fraction on the effective viscosity is investigated. Clearly, at a larger volume fraction, a larger effective viscosity is predicted both for MGA as well as EMA. It is evident that, for

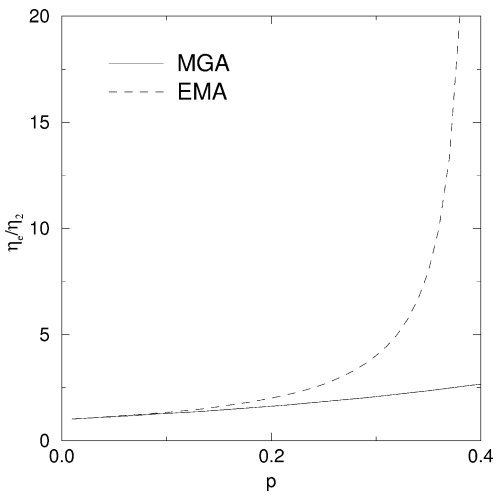

Fig. 2. The MGA and EMA effective viscosity of suspension plotted versus volume fraction p.

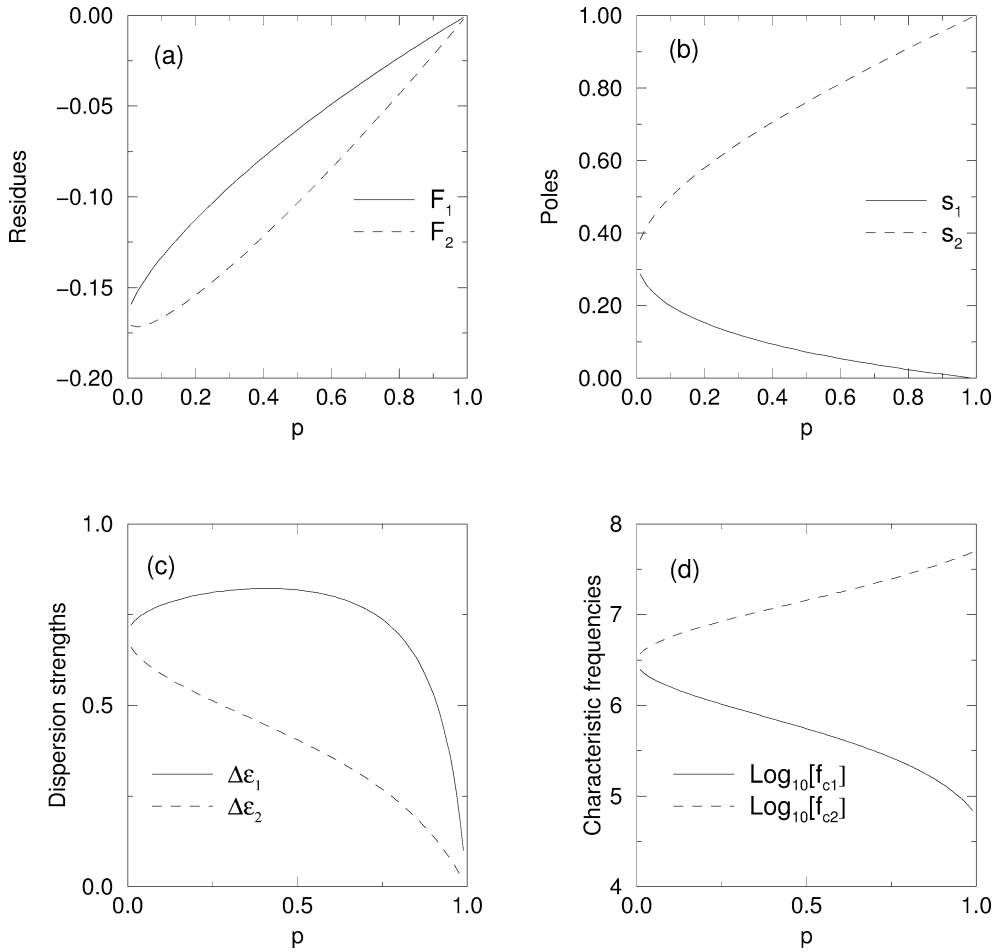

Fig. 3. The spectral parameters F_1, F_2, s_1 and s_2, as well as the dispersion parameters, $\Delta\epsilon_1$ and $\Delta\epsilon_2$, plotted versus volume fraction p (for the MGA only).

a given p, EMA predicts a larger effective viscosity than MGA.

In Fig. 3, we investigate the dependence of the spectral parameters, namely the residues (F_1 and F_2), the poles (s_1 and s_2), as well as the dispersion parameters ($\Delta\epsilon_1$ and $\Delta\epsilon_2$) on the volume fraction p (for MGA only).

In Fig. 3(a) and (b), as the volume fraction p increases, both F_1 and F_2 increase. Increasing volume fraction p leads to decreasing s_1, but increasing s_2. Note that the residues satisfy the relation $F_1 + F_2 = -(1-p)/3$. In the two figures, the distinction between F_1 and F_2, or s_1 and s_2 is quite small at low volume fraction (e.g., $p = 0.05$, 0.1, and 0.15).

In Fig. 3(c), as the volume fraction increases, $\Delta\epsilon_1$ first increases, and then decreases, while $\Delta\epsilon_2$ decreases monotonically. Note $\Delta\epsilon_2$ becomes very close to $\Delta\epsilon_1$ at low concentration region.

In Fig. 3(d), as the volume fraction increases, f_{c1} decreases, while f_{c2} increases concomitantly. Moreover, it is evident that both characteristic frequencies collapse at low concentration region.

From Fig. 3, it is readily concluded that at low volume fraction, the angular-velocity peaks related to two characteristic frequencies are so close that they can almost be seen as overlapped. This is just the reason why only one rotation peak occurs in our figures. We believe that such distinction between

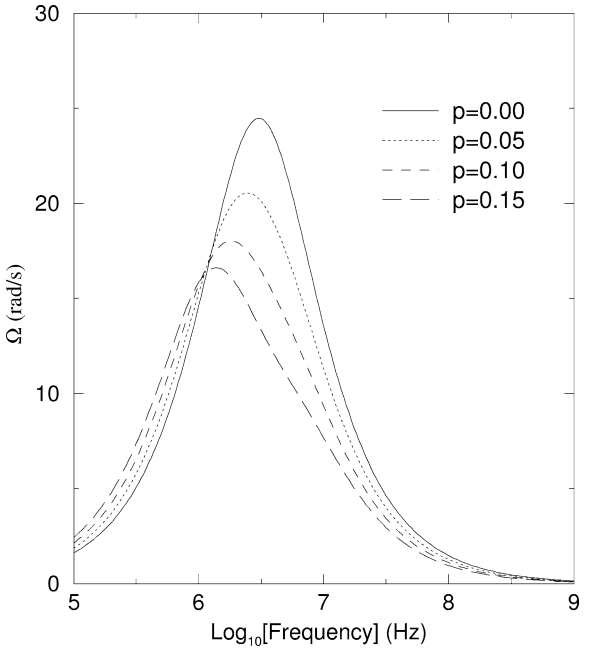

Fig. 4. The rotational angular velocity plotted versus frequency for different volume fraction p. Parameters used in the plot are $\epsilon_1 = 10\epsilon_0, \sigma_1 = 2.8\times10^{-2}$ S/m, $\sigma_2 = 2.8\times10^{-4}$ S/m, $\epsilon_2 = 80\epsilon_0$.

the two peaks will become recognizable for a high-concentration case.

Fig. 4 is plotted for three different volume fraction p at $\sigma_2 = 2.8\times10^{-4}$ S/m, $\epsilon_2 = 80\epsilon_0$, and $\epsilon_1 = 10\epsilon_0$ and $\sigma_1 = 2.8\times10^{-2}$ S/m. In this figure, we investigate the effect of particle volume fraction on the angular velocity. Increasing volume fraction is able to reduce the characteristic frequency as well as the angular-velocity peak value.

4. Discussion and conclusion

Here a few comments on our results are in order. We considered homogeneous, spherical particles exposed to a rotating electric field. As the strength of the rotating electric field increases, the particles in a suspension may be aggregated into sheet-like structures. Within these structures, the concentration of particles is high. In this case, the local-field effect arising from the many-particle system must be taken into account. In this regard, we believe the effective medium theories including both the Maxwell–Garnett approximation (also known as the Clausis–Mossotti approximation) and the effective medium approximation (also known as the Bruggeman approximation) are good candidate theories. The Maxwell–Garnett approximation is well known to be nonsymmetrical and may thus be suitable for low concentration. For a higher concentration of particles, we had better use the effective medium approximation (EMA). Both methods are valid at low concentrations whereas EMA predicts a percolation threshold [10].

We believe our theory will be valid for the case of low Reynolds numbers. In our present study, both the radii and the angular velocities of the particles are small. Thus, we may safely use the effective medium theories for the viscosity, which are valid when the particles are at rest.

We realize the appearance of a circular medium flow because all the particles rotate in the same direction. The macroscopic spin rate may drive the suspending liquid, leading to a decrease of the apparent viscosity of the suspension [13]. Finally, we can apply our formalism to single or multi shell objects, like biological cells [12].

In summary, we have investigated the electrorotation spectrum of many interacting particles including their electric and hydrodynamic interactions. The results showed that the electrorotation spectrum can be modified due to the local field effects arising from the many-particle system. The hydrodynamic interactions between the suspended particles can also modify the spin friction, which is a key to determine the angular velocity of electrorotation. By invoking the spectral representation approach, we derived the analytic expressions for the characteristic frequency at which the maximum angular velocity of electrorotation occurs. We reported a detailed investigation of the dependence of the characteristic frequency and the dispersion strength on various material parameters.

Acknowledgements

This work was supported by the Research Grants Council of the Hong Kong SAR Government under grant CUHK 4245/01P. G.Q.G. acknowledges the financial support from a Key Project of the National Natural Science Foundation of China under grant 19834070. The final version of this Letter was com-

pleted during the Forum on Condensed Matter and Interdisciplinary Physics held at Nanjing University, China on the occasion of the centennial anniversary of the University. K.W.Y. thanks the Organizing Committee for their invitation and the hospitality received from the Laboratory of Solid State Microstructures and the Department of Physics during his stay at the Nanjing University.

References

[1] For a review, see J. Gimsa, D. Wachner, Biophys. J. 77 (1999) 1316.
[2] J. Gimsa, Ann. N.Y. Acad. Sci. 873 (1999) 287.
[3] K. Asami, T. Hanai, N. Koizumi, Jpn. J. Appl. Phys. 19 (1980) 359.
[4] G. Fuhr, J. Gimsa, R. Glaser, Stud. Biophys. 108 (1985) 149.
[5] J. Gimsa, P. Marszalek, U. Lowe, T.Y. Tsong, Biophys. J. 73 (1991) 3309.
[6] G. De Gasperis, X.-B. Wang, J. Yang, F.F. Becker, P.R.C. Gascoyne, Meas. Sci. Technol. 9 (1998) 518.
[7] J.P. Huang, K.W. Yu, G.Q. Gu, Phys. Rev. E 65 (2002) 021401.
[8] K.W. Yu, J.T.K. Wan, Comput. Phys. Commun. 129 (2000) 177.
[9] J. Happel, H. Brenner, Low Reynolds Number Hydrodynamics, Kluwer Academic, Dordrecht/Boston/London, 1983.
[10] T.C. Choy, Physica A 221 (1995) 263.
[11] D.J. Bergman, Phys. Rep. 43 (1978) 379.
[12] J.P. Huang, K.W. Yu, J. Phys. Condens. Matter 14 (2002) 1213; J.P. Huang, K.W. Yu, Commun. Theor. Phys. (2002), in press.
[13] H. Brenner, Ann. Rev. Fluid Mech. 2 (1970) 137.